

Optical Transmission of an Atomic Vapor in the Mesoscopic Regime

T. Peyrot, Y. R. P. Sortais, J.-J. Greffet, and A. Browaeys
*Laboratoire Charles Fabry, Institut d'Optique Graduate School, CNRS,
 Université Paris-Saclay, F-91127 Palaiseau Cedex, France*

A. Sargsyan
Institute for Physical Research, National Academy of Sciences, Ashtarak 2, 0203, Armenia

J. Keaveney, I. G. Hughes, and C. S. Adams
*Department of Physics, Rochester Building, Durham University,
 South Road, Durham DH1 3LE, United Kingdom*

 (Received 24 September 2018; revised manuscript received 8 January 2019; published 20 March 2019)

By measuring the transmission of near-resonant light through an atomic vapor confined in a nanocell we demonstrate a mesoscopic optical response arising from the nonlocality induced by the motion of atoms with a phase coherence length larger than the cell thickness. Whereas conventional dispersion theory—where the local atomic response is simply convolved by the Maxwell-Boltzmann velocity distribution—is unable to reproduce the measured spectra, a model including a nonlocal, size-dependent susceptibility is found to be in excellent agreement with the measurements. This result improves our understanding of light-matter interaction in the mesoscopic regime and has implications for applications where mesoscopic effects may degrade or enhance the performance of miniaturized atomic sensors.

DOI: [10.1103/PhysRevLett.122.113401](https://doi.org/10.1103/PhysRevLett.122.113401)

One important characteristic of mesoscopic systems is the fact that their properties are not ruled by local quantities. The mesoscopic regime arises when the size of the system becomes smaller than a distance ξ characterizing the nonlocal response of the medium to an excitation. Nonlocality is thus a prerequisite to the observation of mesoscopic behaviors. For instance, the concept of local conductivity fails to describe the transport of electrons or phonons when the distance over which the phase of the carriers is lost exceeds the size of the system, as is the case in nanowires [1,2]. In these systems the electrical potential (or the temperature) is undefined and one uses instead a global conductance. Also, nonlocal effects are at the origin of the low temperature anomalous conductivity of a metal at frequencies ranging from GHz to infrared [3], as the skin depth over which the field varies near a surface is smaller than the mean-free path of the electrons in the metal [4,5].

In optics, nonlocality is often observed in *nonlinear* bulk media [6,7], in particular in the presence of long-range interactions between particles [8]. In contrast, manifestations of nonlocal optical properties in *linear* media are scarce. They have been observed for molecules near metallic surfaces [9,10] and the mesoscopic regime was reached with nanoparticles for which the electron mean-free path is on the order of the particle size [11,12]. Also, the *selective reflection* at the interface between a glass and a bulk atomic vapor [13–15] was interpreted as an indirect evidence of nonlocality originating from the motion of

the atoms and their transient response following a collision with the glass surface [16–20]. Confining the vapor in nanocells, i.e., cells with subwavelength thickness, the nonlocality should give rise to a mesoscopic response, as the system size is now on the order of the phase coherence length ξ , as explained below. These nanocells are considered as potential atomic sensors [20,21] and ideal media to explore atom-light [22] and atom-surface interactions [23]. It is therefore important to understand how the mesoscopic response may affect the precision of these sensors. So far, the interplay between nonlocality and system-finite size have been very little studied in nanocells [24] with no comparison between experiment and theory. In particular, the question remains whether the concept of susceptibility holds in this mesoscopic system.

Here, we systematically study the mesoscopic optical response of a hot vapor of cesium confined in a nanocell. We measure the transmission spectra for various cell thicknesses and observe that they cannot be reproduced by a model assuming a local susceptibility. We develop a theoretical model where we calculate explicitly the mesoscopic optical response of the vapor accounting for the nonlocality arising from the motion of the atoms and for the breaking of translational invariance due to the presence of interfaces. In particular, our model defines clearly the parameter regime (velocity, density, and size of the system) where nonlocality dominates in atomic vapors, identifies the role of the system finite-size, and reproduces remarkably well the observed spectra.

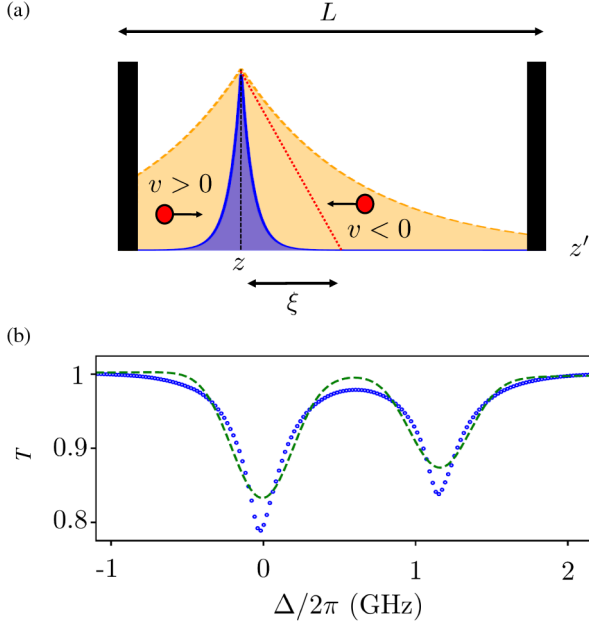


FIG. 1. (a) Illustration of the nonlocal response in the presence of an interface in a slab of thickness L . Orange filled: nonlocal response χ for $\xi \sim L$. Blue filled: local response χ for $\xi \ll L$. (b) Blue line: experimental transmission spectrum for $L = 420$ nm and $\Theta \approx 170^\circ\text{C}$ as a function of the laser detuning Δ with respect to the transition $F = 4$ to $F' = 3$. The data are binned 10 times by steps of 2 MHz. The lines correspond, respectively, to the Cs $D1$ hyperfine transitions $F = 4$ to $F' = 3$ (left), and $F = 4$ to $F' = 4$ (right). Dashed green line: fit by the first local model.

In any *homogeneous* medium, the relation between the polarization vector and the electric field at a frequency ω is given by (one-dimensional model) [25]:

$$P(z, \omega) = \int_{-\infty}^{+\infty} \epsilon_0 \chi(z - z', \omega) E(z') dz', \quad (1)$$

where the susceptibility $\chi(z - z', \omega)$ describes the spatial response of the medium and typically decays over a distance ξ , the so-called range of nonlocality. In an atomic vapor, the nonlocality comes from the motion of the atoms and ξ is equal to their phase coherence length; i.e., the distance traveled by the atoms before the phase of the light excitation imprinted on them is lost (due to collisions with other particles or to radiative decay): $\xi = v/\Gamma_t$ with v the atom velocity and Γ_t the total homogeneous linewidth [16,17,19]. Typically, in a room temperature vapor of alkali, $\xi \approx 3 \mu\text{m}$. In a nanocell, the presence of the walls separated by L breaks the translational invariance [see Fig. 1(a)] and the mesoscopic regime is achieved as soon as $\xi \gtrsim L$. In this regime, the nonlocal relation between P and E [Eq. (1)] also depends on L and the concept of size-independent susceptibility collapses, as is also the case in nanophotonic devices [9,10,26–28].

To observe the mesoscopic optical response resulting from nonlocality, we confine a Cs vapor in a wedged

sapphire nanocell of refractive index $n_s = 1.76$, the thickness of which varies from 30 nm to 2 μm (wedge angle ~ 0.1 mrad) [29,30]. The cell is mounted in a homemade oven that allows differential heating between the reservoir and the windows. The reservoir temperature Θ is monitored by a thermocouple and is related to the atomic density N in the cell via the vapor pressure. An external-cavity diode laser is scanned at 10 Hz around the Cs $D1$ line at $\lambda = 894$ nm (natural linewidth $\Gamma = 2\pi \times 4.6$ MHz) and we use a 7 cm spectroscopic cell as a reference for frequency calibration. The 700 nW laser beam is focused with a waist of $\sim 40 \mu\text{m}$ and scanned along the wedge to explore various thicknesses L of the atomic slab. We use the back reflections on the nanocell to determine L using an interferometric method [31]. Finally, the transmitted light is collected on a photodiode.

When the temperature of the vapor increases, so do the density and the homogeneous linewidth due to collisional dipole-dipole interactions. For $\Theta \geq 250^\circ\text{C}$, we observe linewidths as large as $\Gamma_t = 2\pi \times 1$ GHz leading to $\xi < L$, thus restoring locality [32]. To avoid this situation, we set the temperature of the vapor to a lower value ($\Theta \approx 170^\circ\text{C}$) to keep the expected homogeneous linewidth $\Gamma_t \approx 2\pi \times 60$ MHz [33] such that $\xi > 5L$. Operating at a lower temperature would make the mesoscopic response stronger, at the expense of a much lower absorption, hence reducing the signal-to-noise ratio. The choice of the temperature thus results from a compromise. We present in Fig. 1(b) an example of a transmission spectrum, normalized to the value of the signal far from the atomic resonances, for a thickness of the slab $L = 420$ nm. The line shape appears more complicated than a sum of Gaussian or Lorentzian functions.

In an attempt to model the transmitted spectra, we first use the dispersion theory relying on a description of the vapor (density N) by a *local* susceptibility χ [34]. Specifically, we calculate χ by summing the contributions of all Doppler-broadened hyperfine transitions of the Cs $D1$ line at frequencies $\omega_{FF'}$ [35], assuming a normalized Maxwell-Boltzmann velocity distribution $M_v(v)$ along the laser direction of propagation (d is the dipole moment of the strongest transition, $C_{FF'}$ the Clebsch-Gordan coefficients):

$$\chi(\omega) = \frac{Nd^2}{\hbar\epsilon_0} \sum_{F,F'} C_{FF'}^2 \int_{-\infty}^{\infty} \frac{iM_v(v)}{\Gamma_t - 2i(\Delta_{FF'} - k_l v)} dv. \quad (2)$$

Here, $k_l = 2\pi/\lambda$ is the wave vector of the laser, $\Delta_{FF'} = \omega - \omega_{FF'} - \Delta_p$ and $\Gamma_t = \Gamma + \Gamma_p$, where we have introduced Δ_p and Γ_p a shift and a broadening characterizing the medium, which originates from the collisional dipole-dipole interactions and the atom-surface interactions [30]. The refractive index is then $n(\omega) = \sqrt{1 + \chi(\omega)}$. We account for the multiple reflections inside the cavity formed by the two sapphire plates (index n_s) surrounding the vapor using the transmission function:

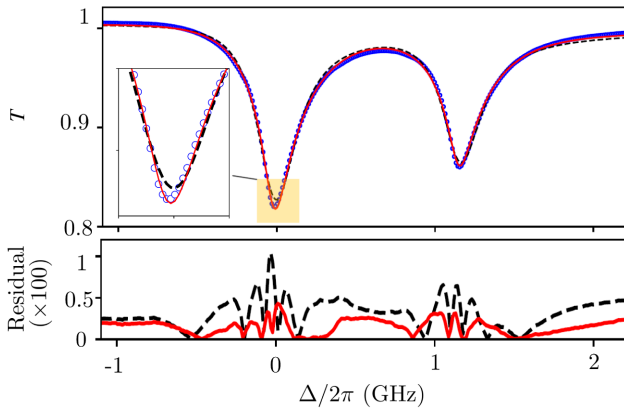


FIG. 2. Top panel. Blue dots: experimental transmission spectrum for $\Theta = 170^\circ\text{C}$ and $L = 360$ nm binned as in Fig. 1(b). Black dot-dashed line: fit by the second model. Red dashed line: fit by the third model (see text). Inset: zoom near resonance. Low panel: absolute value of the residuals for both fits.

$$t(\omega) = \frac{4n_s n \exp[i(n - n_s)k_l L]}{(n_s + n)^2 - (n_s - n)^2 \exp[2ink_l L]}. \quad (3)$$

Finally, we calculate the normalized transmission $T(\omega) = |t[n(\omega)]/t[n = 1]|^2$. The result of this first model is shown in Fig. 1(b), for which we have adjusted the values of N , Δ_p , and Γ_p to best fit the data. Strikingly, it does not agree with the data: the experimental linewidth appears narrower than the calculated Doppler broadened width. This is a signature of the coherent Dicke narrowing already observed by many authors [24,36–38]. In nanocells, this emphasizes the failure of the conventional dispersion theory, which assumes a local susceptibility of the atomic gas and a Maxwell-Boltzmann velocity distribution.

In a second model, we introduce the effect of the cell walls in the simplest possible way: we assume that mainly the atoms flying parallel to the walls contribute to the signal, all the others colliding too rapidly with the walls to participate. We therefore take for the velocity distribution $M_v(v) = \delta(v)$ in Eq. (2) [39], to account phenomenologically for the velocity selection. We fit the data letting as before N , Δ_p , and Γ_p free to evolve. The result, shown in Fig. 2 for $L = 360$ nm, is in much better agreement with the data. Nonetheless, the residuals reveal that the model fails to reproduce the narrow feature near resonance, characteristic of the contribution from the slow atoms [15].

Finally, inspired by previous works [19,41,46], we derive a third, intrinsically nonlocal model that accounts both for the explicit k dependence of the susceptibility and the collisions of the atoms with the surfaces of the nanocell. To do so we first calculate the response function of the atomic medium assuming it is homogeneous and then we account for the influence of the surfaces [10]. The susceptibility in the (k, ω) space of a homogeneous gas of atoms with a velocity v is given, for a specific transition, by [40]

$$\chi_{FF'}(k, \omega, v) = i \frac{d^2 C_{FF'}^2}{\hbar \epsilon_0} \frac{NM_v(v)}{\Gamma_t - 2i(\Delta_{FF'} - kv)}. \quad (4)$$

The k dependence resulting from the Doppler effect is at the origin of the nonlocality and leads to spatial dispersion [25]. Note that this nonlocality is not specific to nanocells, but appears in any atomic vapor. An inverse Fourier transform yields the spatial response function

$$\chi_{FF'}(z - z', \omega, v) = iNM_v(v) \frac{d^2 C_{FF'}^2}{\hbar \epsilon_0 |v|} e^{[-(\Gamma_t/2) + i\Delta_{FF'}][(z - z')/v]} \quad (5)$$

for $(z - z')/v > 0$ and $\chi_{FF'}(z - z', \omega, v) = 0$ for $(z - z')/v < 0$, as required by causality. We recover the above-mentioned decay length $\xi = |v|/\Gamma_t$. As for the influence of the surfaces, we assume quenching collisions with the cell walls [16]; i.e., the phases of the atomic coherences are reset upon collisions. Velocity classes $\pm v$ become independent and the presence of the walls therefore breaks the translational invariance in the medium [47]. We express this fact by multiplying $\chi_{FF'}(z - z', \omega, v)$ by a top-hat function $[\Pi_0^L(z') = 1$ for $0 < z' < L$ and is null elsewhere]. When $\xi \gtrsim L$, the nonlocal response of the medium depends on the size L of the entire system, and is not characteristic of the medium only [see Fig. 1(b)]. Finally, the response of the system is obtained by summing over all the atomic transitions: $\chi_L(z, z', \omega, v) = \sum_{F, F'} \Pi_0^L(z') \times \chi_{FF'}(z - z', \omega, v)$.

To calculate the field transmitted through the cell filled with the vapor, we also consider the multiple reflections inside the cavity formed by the sapphire windows. The transmitted field E_t is the superposition of the field transmitted by the empty cavity E_{t0} , and of the fields E_{t+} and E_{t-} initially scattered by the atoms in the forward and backward directions and that have undergone multiple reflections before being transmitted. The field transmitted by the empty cavity is $E_{t0} = t_1 t_2 / (1 - r_2^2 e^{2ik_l L}) E_0 e^{ik_l z}$ with $t_1 = 2n_s / (1 + n_s)$, $t_2 = 2 / (1 + n_s)$, $r_2 = (1 - n_s) / (1 + n_s)$, and $E_0 e^{ik_l z}$ the incident field. The fields $E_{t+} = E_+$ and $E_{t-} = r_2 E_-$ are related to the polarization vector $P(z, \omega)$ inside the medium by [40]

$$E_{\pm}(z) = \frac{t_2}{1 - r_2^2 e^{2ik_l L}} \frac{ik_l}{2\epsilon_0} \int_0^L dz' P(z', \omega) e^{ik_l(z \mp z')}, \quad (6)$$

where the polarization inside the medium is linked to the total cavity field $E(z)$ by the expression generalizing Eq. (1):

$$P(z', \omega) = \int_{-\infty}^{\infty} dz'' \int_{-\infty}^{\infty} dv \epsilon_0 \chi_L(z', z'', \omega, v) E(z''). \quad (7)$$

The integrals can be calculated [40], assuming the atomic medium to be dilute and thin enough so that the cavity field is approximately the one inside the empty cavity

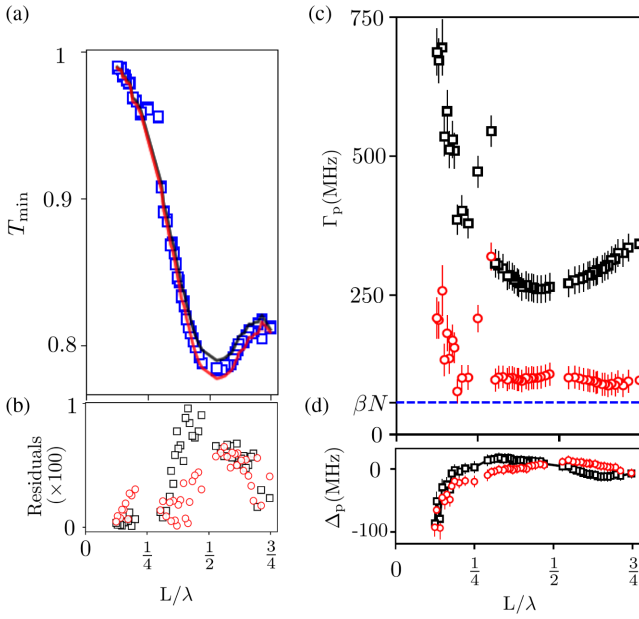


FIG. 3. (a) Minimum of transmission T_{\min} for the transition from $F = 4$ to $F' = 3$ against the cell thickness L . Blue squares: experimental data. Black and red lines: values deduced from the fit of the spectra using the second and third models, respectively. Error bars are smaller than markers. (b) Absolute value of the residuals for the second (black) and third (red) models. (c) (respectively, d): broadening parameter Γ_p (respectively, shift parameter Δ_p) obtained from the fit of the spectra using the second model (black squares) and third model (red circles). Error bars are the quadratic sum of statistic and fit errors. Blue dotted line: collisional broadening prediction [33].

(Born approximation [48]): $E(z'') \approx t_1 / (1 - r_2^2 e^{2ik_i L}) E_0 [e^{ik_i z''} + r_2 e^{ik_i (2L - z'')}]$. Under this assumption, and taking a Maxwell velocity distribution, we compute them numerically to extract the normalized transmission $T(\omega) = |E_t/E_{t0}|^2$. After abandoning the description of the system by a size-independent response function, the transmission is now the global observable characterizing the optical response in our mesoscopic regime. Our approach starting from the nonlocal response function agrees with the formulae obtained in Ref. [41] under the same assumption, i.e., for low absorption.

The fit of the data by the third model is presented in Fig. 2 for the best found parameters N , Δ_p , and Γ_p . The agreement is excellent. In particular, the narrow feature near resonance is reproduced accurately: despite the fact that we keep the full Maxwell velocity distribution, the velocity selection, imposed in the second phenomenological model and at the origin of the narrowing, is an automatic consequence of the third, nonlocal model. To further test the two last models, we also plot in Figs. 3(a) and 3(b) the value T_{\min} of the minimum of the transmission for the hyperfine transition from $F = 4$ to $F' = 3$ as a function of the cell thickness. We observe that both models are in good agreement with the data although the third model fits better

around $L \approx \lambda/2$ [49]. Also, $T_{\min}(L)$ does not decay exponentially as the Beer-Lambert law would predict [34]. This is expected for two reasons. First, the atoms being in a cavity, the transmitted field amplitude is not given by the Beer-Lambert law but by Eq. (3): a $\lambda/2$ -periodic oscillation, originating from the multiple reflections in the cavity, modulates the exponential decay. Second, even without the cavity, the field inside the vapor cannot be exponential due to the nonlocal character of the medium [16], which leads to a λ -periodic oscillation [40].

Even though the residuals in Fig. 2 could discriminate between the second phenomenological and third nonlocal models [50], the values of Δ_p and Γ_p returned by the fit indicate clearly that only the third model is correct, as we now discuss. Both parameters characterize the bulk properties of the vapor and the van der Waals interactions between the atoms and the surfaces. They depend *a priori* on the density N (constant at a given temperature of the vapor) and the cell thickness L . The L dependence comes only from the atom-surface interaction, as for small L the fraction of atoms close to the surface is larger than for large L . For Cs, the theoretical atom-sapphire interaction coefficient C_3 is around a few kHz μm^3 [51,52]: in the range $\lambda/4 \leq L \leq \lambda$ the influence of the surface on Γ_p and Δ_p is therefore expected to be smaller than 10 MHz and thus negligible. Importantly, the cavity effects are already taken into account in both models through the multiple reflections and therefore should not contribute to Γ_p and Δ_p [53]. For a fitting model to make sense, it should therefore return values of Γ_p and Δ_p independent of L . Figure 3(c) shows the values of Γ_p returned by the fit for the two last models as a function of L . Only the third model is able to return a value independent of L for $L \geq 200$ nm. At smaller distances, Γ_p increases due to the atom-surface interaction [40]. Furthermore, for $L \geq 200$ nm, Γ_p is in reasonable agreement with the expected broadening βN due to collisional dipole-dipole interactions at the density corresponding to $\Theta \approx 170^\circ\text{C}$ [33]. The second, phenomenological model, by contrast, yields a strong dependence of Γ_p with L , which is not acceptable based on the arguments presented above. As a consequence the only model, which features both a good agreement with the data and a consistent interpretation of its fitting parameters, is the third one. Figure 3(d) presents the fitted Δ_p against L : the difference between the two models is less striking. Both feature the influence of the attractive atom-surface interaction at small thickness.

The situation studied in this work, of an atomic vapor where the phase coherence length exceeds the dimension of the system, is widely met in miniaturized atomic sensors. We have shown that the propagation of light through nanocells cannot be described by any local property, and even the concept of nonlocal system-size-independent susceptibility collapses. The optical response of mesoscopic systems is now understood globally using a transmission factor. This situation is reminiscent of the electrical conduction in the

mesoscopic regime where the concept of local conductivity is no longer valid and a global conductance has to be introduced. Our model makes explicit the role of nonlocality and its dependence with the system size, and agrees with experimental data for extinctions as large as 20%. To our knowledge, the agreement presented here between theory and experiment is unprecedented in both atomic hot and cold dense atomic vapors altogether [54]. Importantly, it allows the extraction of meaningful quantities such as energy shift and linewidth, hence providing a theoretical framework for characterizing future atomic sensors.

We thank D. Sarkisyan, G. Dutier, A. Laliotis, and D. Bloch for discussions. T. Peyrot is supported by DGA-DSTL Fellowship 2015600028. We also acknowledge financial support from CNRS, EPSRC (Grant No. EP/R002061/1) and Durham University.

-
- [1] N. Agraït, A. L. Yeyatib, and J. M. van Ruitenbeek, Quantum properties of atomic-sized conductors, *Phys. Rep.* **377**, 81 (2003).
- [2] K. Schwab, E. A. Henriksen, J. M. Worlock, and M. L. Roukes, Measurement of the quantum of thermal conductance, *Nature (London)* **404**, 974 (2000).
- [3] A. B. Pippard, The surface impedance of superconductors and normal metals at high frequencies II. The anomalous skin effect in normal metals, *Proc. R. Soc. A* **191**, 385 (1947).
- [4] F. Wooten, *Optical Properties of Solids* (Academic Press, New York, 1972).
- [5] P. W. Gilbert, The anomalous skin effect and the optical properties of metals, *J. Phys. F* **12**, 1845 (1982).
- [6] R. W. Boyd, *NonLinear Optics*, 3rd ed. (Academic Press, New York, 2008).
- [7] C. Rotschild, B. Alfassi, O. Cohen, and M. Segev, Long-range interactions between optical solitons, *Nat. Phys.* **2**, 769 (2006).
- [8] H. Busche, P. Huillery, S. W. Ball, T. Ilieva, M. P. A. Jones, and C. S. Adams, Contactless nonlinear optics mediated by long-range Rydberg interactions, *Nat. Phys.* **13**, 655 (2017).
- [9] C. F. Eagen, W. H. Weber, S. L. McCarthy, and R. W. Therhune, Time-dependent decay of surface-plasmon-coupled molecular fluorescence, *Chem. Phys. Lett.* **75**, 274 (1980).
- [10] G. W. Ford and W. H. Weber, Electromagnetic interactions of molecules with metal surfaces, *Phys. Rep.* **113**, 195 (1984).
- [11] U. Kreibig and L. Genzel, Optical absorption of small metallic particles, *Surf. Sci.* **156**, 678 (1985).
- [12] Ch. Voisin, N. Del Fatti, D. Christofilos, and F. Vallée, Ultrafast electron dynamics and optical nonlinearities in metal nanoparticles, *J. Phys. Chem. B* **105**, 2264 (2001).
- [13] J. L. Cojan, Contribution à l'étude de la réflexion sélective sur les vapeurs de mercure de la radiation de résonance du mercure, *Ann. Phys. (Berlin)* **12**, 385 (1954).
- [14] A. L. J. Burgmans, M. F. H. Schuurmans, and B. Bölger, Transient behavior of optically excited vapor atoms near a solid interface as observed in evanescent wave emission, *Phys. Rev. A* **16**, 2002 (1977).
- [15] S. Briaudeau, S. Saltiel, G. Nienhuis, D. Bloch, and M. Ducloy, Coherent Doppler narrowing in a thin vapor cell: Observation of the Dicke regime in the optical domain, *Phys. Rev. A* **57**, R3169 (1998).
- [16] M. F. H. Schuurmans, Spectral narrowing of selective reflections, *J. Phys. (Paris)* **37**, 469 (1976).
- [17] G. Nienhuis, F. Schuller, and M. Ducloy, Nonlinear selective reflection from an atomic vapor at arbitrary incidence angle, *Phys. Rev. A* **38**, 5197 (1988).
- [18] T. A. Vartanyan and F. Träger, Line shape of resonances recorded in selective reflection: Influence of an antireflection coating, *Opt. Commun.* **110**, 315 (1994).
- [19] T. A. Vartanyan and D. L. Lin, Enhanced selective reflection from a thin layer of a dilute gaseous medium, *Phys. Rev. A* **51**, 1959 (1995).
- [20] R. Ritter, N. Gruhler, H. Dobbertin, H. Kübler, S. Scheel, W. Pernice, T. Pfau, and R. Löw, Coupling Thermal Atomic Vapor to Slot Waveguides, *Phys. Rev. X* **8**, 021032 (2018).
- [21] S. Knappe, P. D. D. Schwindt, V. Shah, L. Hollberg, J. Kitching, L. Liew, and J. Moreland, A chip-scale atomic clock based on ^{87}Rb with improved frequency stability, *Opt. Express* **13**, 1249 (2005).
- [22] J. Keaveney, I. G. Hughes, A. Sargsyan, D. Sarkisyan, and C. S. Adams, Maximal Refraction and Superluminal Propagation in Gaseous Nanolayer, *Phys. Rev. Lett.* **109**, 233001 (2012).
- [23] A. Sargsyan, A. Papoyan, I. G. Hughes, C. S. Adams, and D. Sarkisyan, Selective reflection from an Rb layer with a thickness below $\lambda/12$ and applications, *Opt. Lett.* **42**, 1476 (2017).
- [24] G. Dutier and M. Ducloy, Collapse and revival of a Dicke-type coherent narrowing in a sub-micron thick vapor cell transmission spectroscopy, *Europhys. Lett.* **63**, 35 (2003).
- [25] L. D. Landau, L. P. Pitaevskii, and E. M. Lifshitz, *Electrodynamics of Continuous Media*, 2nd ed. (Pergamon Press, New York, 1984).
- [26] G. H. Coccoletzi and W. L. Mochán, Excitons: From excitations at surfaces to confinement in nanostructures, *Surf. Sci. Rep.* **57**, 1 (2005).
- [27] R. J. Churchill and T. G. Philbin, Electromagnetic reflection, transmission, and energy density at boundaries of nonlocal media, *Phys. Rev. B* **94**, 235422 (2016).
- [28] C. Tserkezis, N. A. Mortensen, and M. Wubs, How nonlocal damping reduces plasmon-enhanced fluorescence in ultranarrow gaps, *Phys. Rev. B* **96**, 085413 (2017).
- [29] D. Sarkisyan, D. Bloch, A. Papoyan, and M. Ducloy, Sub-doppler spectroscopy by sub-micron thin Cs vapor layer, *Opt. Commun.* **200**, 201 (2001).
- [30] T. Peyrot, Y. R. P. Sortais, A. Browaeys, A. Sargsyan, D. Sarkisyan, J. Keaveney, I. G. Hughes, and C. S. Adams, Collective Lamb Shift of a Nanoscale Atomic Vapor Layer within a Sapphire Cavity, *Phys. Rev. Lett.* **120**, 243401 (2018).
- [31] E. Jahier, J. Guéna, Ph. Jacquier, M. Lintz, A. V. Papoyan, and M. A. Bouchiat, Temperature-tunable sapphire windows for reflection loss-free operation of vapor cells, *Appl. Phys. B* **71**, 561 (2000).
- [32] We used this possibility in our measurement of the collective Lamb shift in a dense vapor [30].

- [33] L. Weller, R. J. Bettles, P. Siddons, C. S. Adams, and I. G. Hughes, Absolute absorption on the rubidium $D1$ line including resonant dipole-dipole interactions, *J. Phys. B* **44**, 195006 (2011).
- [34] C. S. Adams and I. G. Hughes, *Optics f2f* (Oxford University Press, Oxford, 2019).
- [35] M. A. Zentile, J. Keaveney, L. Weller, D. J. Whiting, C. S. Adams, and I. G. Hughes, ElecSus: A program to calculate the electric susceptibility of an atomic ensemble, *Comput. Phys. Commun.* **189**, 162 (2015).
- [36] R. Dicke, The effect of collisions upon the Doppler width of spectral lines, *Phys. Rev.* **89**, 472 (1953).
- [37] R. H. Romer and R. Dicke, New technique for high-resolution microwave spectroscopy, *Phys. Rev.* **99**, 532 (1955).
- [38] A. Sargsyan, Y. Pashayan-Leroy, C. Leroy, and D. Sarkisyan, Collapse and revival of a Dicke-type coherent narrowing in potassium vapor confined in a nanometric thin cell, *J. Phys. B* **49**, 075001 (2016).
- [39] We also consider in the Supplemental Material [40] the case of a bimodal distribution. The main conclusions of the paper are unchanged, but the price to pay is the introduction of two extra fitting parameters.
- [40] See Supplemental Material at <http://link.aps.org/supplemental/10.1103/PhysRevLett.122.113401> for more detailed informations, which includes Refs. [5,15,16,19,41–45].
- [41] G. Dutier and M. Ducloy, Revisiting optical spectroscopy in a thin vapor cell: Mixing of reflection and transmission as a Fabry Perot microcavity effect, *J. Opt. Soc. Am. B* **20**, 793 (2003).
- [42] G. Grynberg, A. Aspect, and C. Fabre, *Introduction to Quantum Optics* (Cambridge University Press, New York, 2010).
- [43] H. Fearn, D. F. V. James, and P. Milonni, Microscopic approach to reflection, transmission and the Ewald-Osen extinction theorem, *Am. J. Phys.* **64**, 986 (1996).
- [44] R. P. Feynman, R. B. Leighton, and M. Sands, *Lectures on Physics* (Addison Wesley, Reading, MA, 2006), Vol. 1, Chap. 30.
- [45] K. A. Whittaker, J. Keaveney, I. G. Hughes, A. Sargsyan, D. Sarkisyan, and C. S. Adams, Spectroscopic detection of atom-surface interactions in an atomic-vapor layer with nanoscale thickness, *Phys. Rev. A* **92**, 052706 (2015).
- [46] B. Zambon and G. Nienhuis, Reflection and transmission of light by thin vapor layers, *Opt. Commun.* **143**, 308 (1997).
- [47] This is in contrast to the case of elastic collisions at the wall [40].
- [48] R. Carminati and J.-J. Greffet, Influence of dielectric contrast and topography on the near field scattered by an inhomogeneous surface, *J. Opt. Soc. Am. A* **12**, 2716 (1995).
- [49] The odd behavior of the data around $L \simeq \lambda/4$, already pointed out in J. Keaveney, A. Sargsyan, U. Krohn, I. G. Hughes, D. Sarkisyan, and C. S. Adams, Cooperative Lamb Shift in an Atomic Vapor Layer of Nanometer Thickness, *Phys. Rev. Lett.* **108**, 173601 (2012) in a different context, is not understood and will be the subject of future investigations.
- [50] I. G. Hughes and T. P. A. Hase, *Measurements and Their Uncertainties: A Practical Guide to Modern Error Analysis* (OUP, Oxford, 2010).
- [51] K. A. Whittaker, J. Keaveney, I. G. Hughes, A. Sargsyan, D. Sarkisyan, and C. S. Adams, Optical Response of Gas-Phase Atoms at Less Than $\lambda/80$ From a Dielectric Surface, *Phys. Rev. Lett.* **112**, 253201 (2014).
- [52] D. Bloch and M. Ducloy, Atom-wall interaction, *Adv. At. Mol. Opt. Phys.* **50**, 91 (2005).
- [53] For the dilute vapor used here, the residual oscillatory dependence of Δ_p with L observed in [30] has an amplitude lower than 10 MHz, and is therefore negligible.
- [54] S. Jennewein, L. Brossard, Y. R. P. Sortais, A. Browaeys, P. Cheinet, J. Robert, and P. Pillet, Coherent scattering of near-resonant light by a dense, microscopic cloud of cold two-level atoms: Experiment versus theory, *Phys. Rev. A* **97**, 053816 (2018).